ELSEVIER

www.elsevier.nl/locate/carres

Carbohydrate Research 331 (2001) 291–306

CARBOHYDRATE RESEARCH

Purification and characterisation of a galactoglucomannan from kiwifruit (*Actinidia deliciosa*)

Roswitha Schröder,[a] Pierre Nicolas,[b] Sébastien J.F. Vincent,[b] Monica Fischer,[b] Sylviane Reymond,[b] Robert J. Redgwell[b,*]

[a] *HortResearch, Mount Albert Research Centre, Private Bag 92169, Auckland, New Zealand*
[b] *Nestlé Research Center, Nestec Ltd., Vers-chez-les-Blanc, PO Box 44, CH-1000, Lausanne 26, Switzerland*

Received 13 November 2000; accepted 2 February 2001

Abstract

A galactoglucomannan (GGM) has been purified from the primary cell walls of ripe kiwifruit. A combination of barium hydroxide precipitation, anion exchange- and gel-permeation chromatography gave a chemically homogeneous polymer with a 1:2:2 galactose–glucose–mannose ratio and a molecular weight range of 16–42 kDa. Complete hydrolysis of the polymer with *endo*-1,4-β-mannanase (EC 3.2.1.78) from *Aspergillus niger* gave a mixture of oligosaccharides, three of which (**II**, **III**, **IV**) accounted for more than 80% of the GGM. Structural characterisation of these oligosaccharides and the original polysaccharide was achieved by linkage analysis, 1D and 2D NMR spectrometry and enzymatic hydrolysis. Oligosaccharide **II** β-D-Glc*p*-(1→4)-β-D-Man*p*-(1→, **III** β-D-Glc*p*-(1→4)-[α-D-Gal*p*-(1→6)]-β-D-Man*p*-(1→, and **IV** β-D-Glc*p*-(1→4)-[β-D-Gal*p*-(1→2)-α-D-Gal*p*-(1→6)]-β-D-Man*p*-(1→4)-β-D-Glc*p*-(1→4)-β-D-Man*p*-(1→, appeared in the molar ratio of 2:1:1. A trace amount of mannobiose (**I**) was detected, indicating that some of the mannosyl residues were contiguous. It is concluded that the predominant structural feature of kiwifruit GGM is a backbone of alternating β-(1→4)-linked D-glucopyranosyl and D-mannopyranosyl residues, with approximately one third of the latter carrying side-chains at O-6 of single α-D-Gal*p*-(1→ residues (50% of the branches) or the disaccharide β-D-Gal*p*-(1→2)-α-D-Gal*p*-(1→ (50% of the branches), the substituted residues being separated by three or five unsubstituted monosaccharide units.

Keywords: *Actinidia deliciosa*; Galactoglucomannan; Plant primary cell wall; NMR spectroscopy; Linkage analysis; Kiwifruit; Oligosaccharides; Polysaccharide

1. Introduction

The non-cellulosic polysaccharides xyloglucan, galactoglucomannan and glucuronoarabinoxylan are widespread components of the primary cell wall of many plants.[1] Most interest has focused on the xyloglucans (XG), which are well characterised and have a clear structural role in the skeletal framework of the wall. Evidence that xyloglucans act as an inter-molecular tether between cellulose fibrils is based on their well-documented ability to hydrogen bond to cellulose[2] and the discovery of the enzyme xyloglucan endotransglycosylase (XET), which potentially can hydrolyse and rejoin xyloglucan chains to accommodate cell growth and expansion.[3,4]

In contrast to the xyloglucans, the galactoglucomannans (GGM) have attracted less

* Corresponding author. Tel.: +41-21-7858681; fax: +41-21-7858554.
E-mail address: robert.redgwell@rdls.nestle.com (R.J. Redgwell).

0008-6215/01/$ - see front matter
PII: S0008-6215(01)00046-5

attention. They are less widely characterised and no clear role for them has been established within the overall architecture of the wall despite their presence throughout the plant kingdom. GGMs have been found in mosses,[5] ferns,[6] secondary walls of gymnosperms[7,8] and angiosperms,[9] and primary walls of monocots[10] and dicots.[11–13] All GGMs are characterised by a backbone of β-D-Glc*p*-(1→4) and β-D-Man*p*-(1→4) residues, with the latter substituted at O-6 with D-Gal*p* residues. The reported ratio of Gal–Glc–Man varies, depending on the plant source and developmental stage of the tissue.

Many of the characterised GGMs originated from suspension cultured cells which not only provide a continuous source of polysaccharide but the polymers are often secreted into the medium, making their isolation simpler.[14–17] One of the more recent detailed structural characterisations was of the GGM secreted into a medium of suspension-cultured cells of *Nicotiana plumbaginifolia*.[18] The GGM backbone was predominantly alternating β-D-Glc*p*-(1→4) and β-D-Man*p*(1→4) residues with the latter substituted at O-6 with either single α-D-Gal-(1→ residues or the disaccharide β-D-Gal*p*-(1→2)-α-D-Galp-(1→. For the first time, small amounts of arabinose and xylose were shown to be covalent constituents of the GGM, attached at O-6 of the →4)-β-D-Man*p*-(1→ residues.

Whereas suspension-cultured cells provide a convenient source of cell walls, the structural features of a particular polysaccharide isolated from suspension cultures may not necessarily be the same as those found in the whole plant from which the cells were derived. We previously compared the structural details of a GGM fraction isolated from the outer pericarp of kiwifruit (*Actinidia deliciosa)* and from suspension-cultured cells prepared from the same tissue.[13] The GGM from the cultured cells possessed a Gal–Glc–Man ratio of approximately 1:1:1 whereas for the GGM from the outer pericarp tissue the ratio was 0.5:1:1. The reported Gal–Glc–Man ratios for the GGM of suspension-cultured cells of *N. plumbaginifolia*,[18] *Nicotiana tabacum*,[16] *Rubus fruticosus*,[15] and *A. deliciosa*[13] are all very similar. This implies that there were greater differences in the structural features of GGM between a plant tissue and its corresponding suspension-cultured cells, than between GGM from different types of plant. More information is therefore required on the structural features of GGM isolated from primary cell walls of whole plants.

One of several problems in attempting to isolate and purify GGM from whole fruit tissue is the insolubility of the GGM, possibly due to its close association with the xyloglucan and/or the cellulose fibrils. It is also difficult to remove contaminating pectin and xyloglucan that are present in the primary cell wall at much higher concentrations than the GGM. In this paper, we report on a method for the isolation and purification of a GGM from kiwifruit outer pericarp that minimises these problems and the elaboration of its structural features by enzymatic hydrolysis, methylation analysis and ^{1}H and ^{13}C NMR spectroscopy.

2. Experimental

General.—Polysaccharides were hydrolysed with 2 M CF_3COOH for 1 h at 110 °C. Sugar mixtures were converted into alditol acetates for GLC analysis as described by Fischer et al.[13] Polysaccharides and oligosaccharides were methylated using a modification of the method of Ciucanu and Kerek.[19] GLC–MS of the partially methylated alditol acetates was accomplished as described previously.[13] Carbohydrate content was quantified by the phenol–H_2SO_4 method of Dubois et al.[20]

Purification of GGM

Isolation of crude non-cellulosic polysaccharides fraction from OP. Ripe kiwifruit (approx. 0.2–0.5 kg firmness) were purchased from the local supermarket. Outer pericarp (6 kg) was excised from the fruit and immediately homogenised in 200 g portions with 400 mL ice-cold water using a Waring blender. Homogenates were centrifuged (6000*g*, 10 min, 4 °C for all centrifugation steps), and the supernatant decanted. The residue was re-suspended in ice-cold water and re-centrifuged. The residue was then homogenised in 70:2.5:2.5:25 EtOH–HOAc–$CHCl_3$–water (4

L), centrifuged and sequentially extracted with water (4 L, ambient temperature), 0.05 M *trans*-1,2-diaminocyclohexane-*N*,*N*,*N*′,*N*′-tetraacetic acid (CDTA) in 1 M KOH containing 20 mM $NaBH_4$ (4 L, 1 h, ambient temperature), and 4 M KOH containing 20 mM $NaBH_4$ (4 L, 4 h, ambient temperature). The 4 M KOH supernatant containing non-cellulosic polysaccharides (XG, GGM and pectin) was recovered by centrifugation, neutralised with HOAc, concentrated and dialysed (molecular weight cut-off 12 kDa).

Removal of pectic polysaccharides.—Hexadecyltrimethylammoniumbromide (CTAB, 1%) was added to the 4 M KOH-soluble fraction in equal volumes and the solution left overnight at ambient temperature. The precipitate containing pectic polysaccharides was removed by centrifugation. The supernatant containing predominantly XG and GGM was shaken four times with amounts of $CHCl_3$ to remove CTAB. The aqueous phase was dialysed against 20% EtOH for 2 days at ambient temperature followed by water for 5 days at 4 °C (molecular weight cutoff (MWCO) 12 kDa).

Removal of xyloglucan.—NaOH was added to the dialysate to a final concentration of 5% and an equivalent volume of freshly prepared 5% $Ba(OH)_2$ was added. After 1 h at rt, the solution was centrifuged and the pellet containing GGM was washed with 5% $Ba(OH)_2$ to remove contaminating XG. The pellet was dissolved in 5% NaOH, neutralised with HOAc and dialysed (MWCO 3.5 kDa). The dialysate was concentrated to 30 mL (total polysaccharide content approx. 800 mg) and stored in 1 mL aliquots at −20 °C until further purification by gel-permeation chromatography.

Gel-permeation chromatography.—Aliquots were loaded on Sephacryl S-300 (90 × 2 cm bed, eluent 0.05 M AcONa pH 6.0, 0.125 M NaCl, 0.05% chlorobutanol, flow rate 6 mL h^{-1}, 30 min fractions). Fractions 44–60 were pooled, dialysed (MWCO 3.5 kDa), concentrated and subjected to borate anion-exchange chromatography.

Anion-exchange chromatography.—A column of DEAE-Sepharose (2.5 × 11 cm) was equilibrated with 30 mM sodium borate buffer (pH 9.0). Borate buffer (1 M, pH 9.0) was added to GGM fractions to a final concentration of 30 mM and loaded onto the column followed by 30 mM buffer to remove unbound polysaccharides. Elution was monitored by the phenol–H_2SO_4 assay. When the eluate was phenol–H_2SO_4 negative, polysaccharides retained on the column were eluted with a borate buffer gradient (30 mM–1 M, 100 mL each; flow rate 35 mL h^{-1}). The phenol–H_2SO_4 positive fractions (10–15) were pooled, dialysed (MWCO 3.5 kDa) and re-chromatographed on Sephacryl S-300. Fractions 44 to 60 were pooled, dialysed and freeze-dried. The final yield of GGM was 220 mg.

Molecular weight determination of GGM by dynamic laser light scattering spectrometry.—Pure GGM (7.5 mg) was dissolved in 1 mL water and separated by gel-permeation chromatography on Sephacryl S-300. Fractions eluted at the beginning, middle and end of the peak were pooled, dialysed against water (MWCO 3.5 kDa), and freeze-dried. Fractions were re-dissolved in 100–150 μL water, stirred for 72 h at 4 °C, and filtered through Millipore filters (0.22 μm pore size). Prior to molecular weight determination by dynamic laser-light scattering (DynaPro 2001™), samples were centrifuged (10 min, 10,000*g*, ambient temperature). Pullulans and dextrans (T2000, T70, T40, T10; purified by gel-permeation chromatography on appropriate columns) were used as calibration standards. Molecular weight averages were obtained after 20 measurements at rt.

Purification of oligosaccharides generated by enzymatic digestion of GGM for molecular weight determination, linkage and NMR analysis.—GGM (40 mg) was dissolved in 7 mL 1:1:98 HOAc–pyridine–water buffer, pH 4.7. *endo*-1,4-β-Mannanase from *A. niger* (100 U, Megazyme, Ireland, 297 U mL^{-1}) was added and the mixture incubated at 37 °C overnight.

Gel-permeation chromatography.—Oligosaccharides were separated on Toyopearl HWS40 (1.5 × 170 cm, eluent 98:1:1, HOAc–pyridine–water, flow rate 4.5 mL h^{-1}, 30 min fractions). Elution was monitored by the phenol–H_2SO_4 assay. Peaks were pooled according to elution profile (peak **IV** fractions

62–66, peak **III** fractions 70–74, peak **II** fractions 76–80), concentrated and re-chromatographed on the same column. Examination by HPTLC showed each oligosaccharide fraction contained a single component following the second gel-permeation chromatographic step, and they were therefore considered sufficiently pure for molecular weight determination, linkage and NMR analysis.

High-performance anion-exchange chromatography (HPAEC-PAD).—Oligosaccharides from enzyme-treated GGM were dissolved in de-ionised water (1 mg mL^{-1}) and separated by HPAEC on a Dionex BioLC (Dionex USA) using a CarboPac PA-1 column (4 × 250 mm) equilibrated in 150 mM NaOH. Elution was done with a linear gradient of NaOAc (0–250 mM) in 150 mM NaOH and oligosaccharide monitored by pulsed amperometric detection (Dionex).

Mass spectrometry of the underivatised oligosaccharides.—The mass spectrometry analyses were carried out using a Micromass AutoSpec OA-TOF mass spectrometer working with an electrospray interface. The samples were dissolved in 6:4 CH_3OH–water acidified with 1% HOAc and infused in the continuous mode at a flow rate of 10 μL min^{-1} through a Harvard model 22 syringe pump. The spray needle was maintained at 4000 V and nitrogen was used separately as both bath and nebulizer gas with flow rates of 400 and 12 L h^{-1}, respectively. The bath gas was maintained at 80 °C. Spectra were acquired in positive mode from 20 to 1000 Da.

NMR spectroscopy.—The three oligosaccharide samples, **II**, **III**, **IV**, were dissolved in 99.96 atom% D_2O (Euriso-Top), while the GGM polysaccharide sample was first dissolved in 99.9 atom% D_2O (Euriso-Top), freeze-dried before being dissolved in 99.96 atom% D_2O (Euriso-Top). All experiments were recorded on a Bruker DRX 600 MHz three-channel NMR spectrometer using an inverse triple-resonance probe equipped with pulsed-field gradients. Chemical shifts are expressed in ppm by reference to the α-anomeric signal of external [^{13}C-1]-D-glucose ($\delta_{H\text{-}1}$ 5.15 and $\delta_{C\text{-}1}$ 92.90).

The following phase-sensitive two-dimensional experiments were recorded for each of the four samples using TPPI,[22] DQF-COSY,[23,24] TOCSY[25] with mixing times between 10 and 90 ms, NOESY[26,27] with mixing times between 50 and 400 ms, gradient sensitivity-enhanced ^{13}C–^{1}H HSQC,[28] together with absolute mode gradient-filtered ^{13}C–^{1}H HMBC[29] experiments with *J*-evolution times between 50 and 80 ms. The number of complex points in ($F_1 \times F_2$) were either 1024 × 2048 (COSY, TOCSY and NOESY), or 512 × 2048 (HSQC and HMBC), with 16 scans (COSY, TOCSY and HSQC), 64 scans (NOESY), or 256 scans (HMBC). Spectral widths ($\omega_1 \times \omega_2$) were either 4800 × 4800 Hz (COSY, TOCSY and NOESY) or 7546 × 4800 Hz (HSQC and HMBC). A 90° shifted square sine-bell was used in all cases, with zero-filling once. All data were processed using Bruker XWINNMR 2.6 software.

*Purification and enzymatic analysis of oligosaccharides **IV** and **V**.*—GGM (2 mg) was incubated with *endo*-1,4-β-mannanase in 50 mM NaOAc (400 μL, pH 5.0) at 30 °C for 4 h. Aliquots of the digested material were applied to HPTLC pre-coated plates (Silica Gel 60, E. Merck, Darmstadt, Germany) as a narrow band. The plates were developed three times using 30:35:11 $CHCl_3$–HOAc–water at rt. The zone ends of the bands were detected using the colour reagent described by Hansen[21] and oligosaccharides **IV** and **V** extracted from the plates using 80% EtOH (3 ×).

*Enzymatic analysis of oligosaccharide **IV**.*—Oligosaccharide **IV** (~ 10 μg) was dissolved in 50 mM NaOAc (10 μL, pH 5.0) and incubated with either α-D-galactosidase from green coffee beans (0.10 U, Sigma), or β-D-galactosidase from *Aspergillus niger* (0.10 U, Megazyme), or with a combination of both enzymes at 30 °C for 5 h. The reaction products (oligosaccharides **VI** and **VIII**) were separated by TLC, detected and extracted as described above. Oligosaccharide **IV** (~ 5 μg), oligosaccharide **VI** (~ 5 μg) and oligosaccharide **VIII** (~ 2 μg) were incubated with *endo*-1,4-β-mannanase (0.125 U) in 50 mM NaOAc (5 μL, pH 5.0) at 30 °C for 5 h. The reaction products were separated by TLC and detected as described above.

Enzymatic analysis of oligosaccharide V.—Oligosaccharide **V** (~ 2 μg) was dissolved in 50 mM NaOAc (5 μL, pH 5.0) and incubated with either β-D-galactosidase from *A. niger* (0.10 U) alone or in combination with *endo*-1,4-β-mannanase from *A. niger* (0.125 U) at 30 °C for 5 h. The reaction products (oligosaccharide **VII**, oligosaccharide **III**) were separated by TLC and detected as described above.

3. Results and discussion

Purification, composition and molecular weight determination of galactoglucomannan (GGM) polysaccharide.—GGM was extracted from the outer pericarp of ripe kiwifruit and purified using a combination of barium hydroxide precipitation,[30] gel-filtration and borate anion-exchange chromatography.[31]

The protocol for the isolation of GGM was designed to obviate problems that can arise when purifying the polysaccharide from the primary cell wall of a dicotyledonous plant. These include the fact that GGM preparations often contain trace amounts of pectic polysaccharides and xyloglucan that are more abundant wall components. In addition, GGM is very difficult to remove from the cell wall, and appears to be as strongly bonded to other wall components as xyloglucan (if not more so). To increase the yield of extractable GGM, ripe kiwifruit were used because cell wall loosening was well advanced due to the degradation of pectic polysaccharides.[32] Freeze drying of mixtures of polysaccharides at different stages of purification can cause aggregation of different polymer types making subsequent solubilisation and purification difficult. Therefore, from the initial homogenisation of the fruit, until the final purification step, GGM containing fractions were maintained in either aqueous solution or as hydrated residues.

Barium hydroxide is generally used for precipitating mannose-containing polysaccharides. The crude GGM recovered as a barium hydroxide precipitate contained fucose, arabinose and xylose (up to 7.5 mol.%, Table 1), indicating contamination of the precipitate with XG and/or pectin. After gel-filtration on Sephacryl S-300, the polymer contained galactose (20.6 mol.%), glucose (39.7 mol.%) and mannose (38 mol.%). Fucose, arabinose and xylose were still present in small amounts (1.7 mol.% in total). The high degree of polydispersity with regard to molecular mass of GGM and XG means that there is always some overlap during gel-permeation chromatography, even though the average molecular weight of each polysaccharide is quite different. The GGM was therefore purified using borate anion exchange chromatography. Unlike XG, GGM as a borate complex is retained on the DEAE-Sepharose and can be eluted using a borate gradient. Following anion-exchange chromatography, the fucose, arabinose and xylose content of the GGM was 1 mol.%. The changing composition of fucose, arabinose and xylose during the purification procedure indicated contamination of the preparation with XG and pectin rather than the monomers being structural components of the GGM. This was verified by re-chromatography of the polymer on Sephacryl S-300 after borate anion exchange chromatography. The

Table 1
Monosaccharide composition of GGM (mol.%) at different stages of purification

Sugar	$Ba(OH)_2$-precipitate	Gel-permeation chromatography S-300	Borate anion-exchange chromatography	Re-chromatography S-300
Fuc	0.4	0.4	0.4	tc [a]
Ara	0.5	0.3	0.4	tc [a]
Xyl	6.6	1.0	0.2	tc [a]
Man	31.6	38.0	37.0	38.4
Gal	16.2	20.6	21.7	20.0
Glc	44.7	39.7	40.3	41.6

[a] tc = trace.

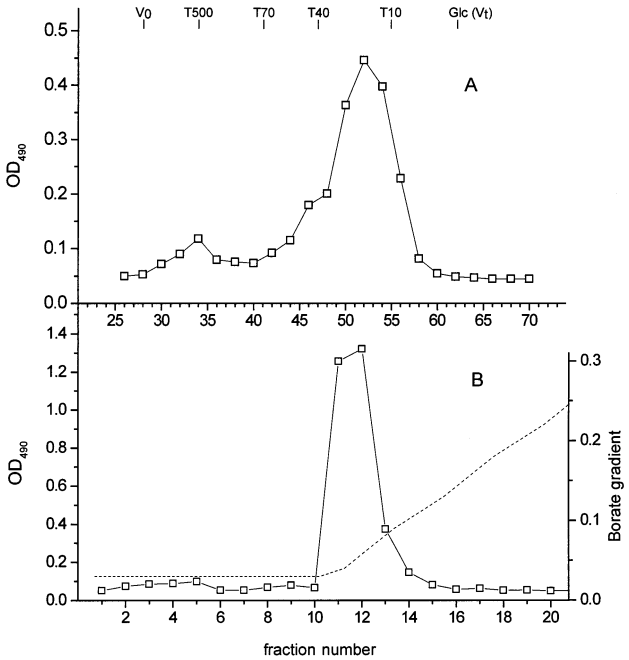

Fig. 1. (A) Gel-permeation chromatography on Sephacryl S-300 of crude GGM from ripe kiwifruit. The column was calibrated with a series of dextrans (T500–T10) and glucose (Glc). (B). Anion-exchange chromatography of GGM on DEAE-Sepharose with sodium borate buffer gradient (pH 9.0).

preparation consisted only of galactose (20 mol.%), glucose (41.6 mol.%) and mannose (38.4 mol.%), with a molar ratio of 0.5:1:0.92. Only trace amounts of fucose, arabinose and xylose could be detected. A typical elution profile of gel-permeation chromatography of the crude GGM extract (A) and anion-exchange chromatography of the GGM fraction as a borate complex (B) is shown in Fig. 1.

The molecular weight (MW) of GGM from kiwifruit was estimated by gel-permeation chromatography and dynamic laser-light scattering spectrometry. Estimated by gel-permeation chromatography using dextrans as MW standards, GGM from ripe kiwifruit had a MW range between 5 and 60 kDa, with the middle of the peak being eluted at approx. 20 kDa (Fig. 1(A)). This is in good agreement with Eda et al.[11] for GGM from midribs of tobacco leaves using the same method. As separation by gel-permeation chromatography not only depends on the size but also the shape of the molecules separated, we have employed dynamic laser-light scattering spectrometry as an additional method to estimate the MW range of GGM from ripe kiwifruit. GGM eluted at the beginning of the peak was estimated to have a MW of 36.4 kDa using pullulans as calibration standards, or 41.8 kDa using purified dextrans as calibration standards. GGM eluted towards the end of the peak had a MW of 16.9 or 17.3 kDa using the same calibration standards. Therefore, the MW range of GGM from ripe kiwifruit determined by dynamic laser-light scattering is approximately between 16.9 and 41.8 kDa. GGM from the middle of the peak proved to be too polydisperse to give a reliable MW determination using this method (data not shown).

Compositional analysis of the three GGM fractions after gel-permeation chromatography gave identical galactose, glucose and mannose ratios across the entire width of the GGM peak, indicating chemical homogeneity (data not shown).

Linkage analysis of GGM polysaccharide.—Linkage analysis of the purified GGM (Table 2) revealed mostly 4-Glc*p*, 4-Man*p*, 4,6-Man*p*, terminal Gal*p* and 2-Gal*p*. These linkage components are consistent with a GGM possessing a (1→4)-glucomannan backbone with approximately one third of the mannose residues substituted at O-6 by galactosyl sidechains. A trace of terminal xylosyl residues was detected but no arabinosyl linkages were identified.

NMR spectroscopy of GGM polysaccharide.—Assignments of the ^{1}H and ^{13}C NMR signals of the GGM at 25 °C are given in Table 3. The 1D ^{1}H NMR spectrum of the GGM polysaccharide (Fig. 2(d)) shows ten major signals in the proton anomeric region. The monosaccharide units were designated **A**–**J** following decreasing anomeric proton chemical shifts. At 25 °C, the GGM exhibited broad lines (linewidths 10 Hz). The HSQC spectra (Fig. 3(d)) confirmed the number of expected monosaccharide units showing ten anomeric resonances. The ^{1}H assignment was started from the anomeric H-1 resonances of each residue in the TOCSY spectra recorded with increasing mixing times (10–90 ms). Connectivities from H-1 to H-2,3,4 were traced for most residues, although overlap, large linewidths and weak signal intensities prevented a complete assignment of the GGM

polysaccharide resonances. Some uncertainties could not be resolved on the basis of additional H-2,3,4 TOCSY traces alone. Therefore assignments were confirmed using intraresidue NOESY cross-peak patterns and by the assignment of HSQC peaks. The assignment was helped by direct comparison of the tentative GGM chemical shifts with those assigned for the three oligosaccharides. The aglyconic carbon positions were identified on the basis of the ^{13}C chemical shifts ($\Delta\delta > +5$ ppm) in comparison with standard monosaccharide methyl glycoside references.[33–35] The glycosidic linkages were deter-

Table 2
Linkage composition of kiwifruit GGM and of three major oligosaccharides formed following *endo*-1,4-β-mannanase treatment of GGM

Sugar	Linkage	Linkage composition (mol.%)			
		GGM	Oligosaccharide **II**	Oligosaccharide **III**	Oligosaccharide **IV**
Xyl*p*	terminal	0.4			
Gal*p*	terminal	16.0		32.1	18.0
	2-	7.5			17.8
Glc*p*	terminal	2.2	57.2	33.2	17.1
	4-	32.0			17.1
	4,6	1.5			
Man*p*	terminal	1.2			
	4-	23.7	42.8		14.1
	4,6-	15.4		34.7	15.8

Table 3
^{1}H and ^{13}C NMR chemical shifts for the GGM polysaccharide[a,b]

	Monosaccharide residue	δ H-1 δ C-1	δ H-2 δ C-2	δ H-3 δ C-3	δ H-4 δ C-4	δ H-5 δ C-5	δ H-6a δ C-6	δ H-6b
A	→2)-α-D-Gal*p*-(1→	5.15 98.9	**3.87** **78.1**	4.09 70.4	3.97 69.6	3.51 75.5	3.76 61.3	3.69
B	→4)-β-D-Man-(1→	5.10 94.2	3.91 70.7	3.69 71.9	**3.89** **78.1**	3.75 71.5	3.94 60.6	3.85
C	α-D-Gal*p*-(1→	4.95 99.2	3.75 71.9	3.89 71.5	3.69 76.9	3.94 69.6	3.84 60.4	3.68
D	→4,6)-β-D-Man*p*-(1→	4.68 100.4	3.98 70.9	4.09 70.4	**3.87** **78.1**	3.86 69.6	**3.92** **68.6**	**3.84**
E	→4,6)-β-D-Man*p*-(1→	4.68 100.4	3.98 71.2	4.09 70.3	3.87 78.1	3.86 69.6	**3.76** **68.6**	**3.74**
F	β-D-Gal*p*-(1→	4.54 103.0	3.54 71.3	3.60 73.0	3.87 71.2	3.48 75.3	3.69 61.5	3.69
G	→4)-β-D-Glc*p*-(1→	4.49 105.0	3.55 71.4	3.59 73.0	**3.85** **78.1**	3.67 71.9	3.82 60.4	3.64
H	→4)-β-D-Glc*p*-(1→	4.45 102.8	3.28 73.2	3.63 75.3	**3.60** **78.9**	3.72 71.9	3.84 60.5	3.68
I	→4)-β-D-Glc*p*-(1→	4.44 102.9	3.29 73.3	3.62 75.3	**3.61** **78.9**	3.55 71.4	3.85 60.5	n.d. [c]
J	→4)-β-D-Glc*p*-(1→	4.42 102.9	3.24 73.6	3.43 73.2	**3.63** **78.9**	3.34 73.2	3.86 60.5	n.d. [c]

[a] Values were determined in D_2O at 25 °C and are given in ppm relative to external [^{13}C-1]-D-glucose ($\delta_{H\text{-}1(\alpha)}$ 5.15 and $\delta_{C\text{-}1(\alpha)}$ 92.90).

[b] Chemical shifts highlighted in bold typeface indicate positions at which a glycosidic link is identified based on differences to the corresponding reference chemical shifts. [33–35]

[c] 'n.d.' stands for 'not determined'.

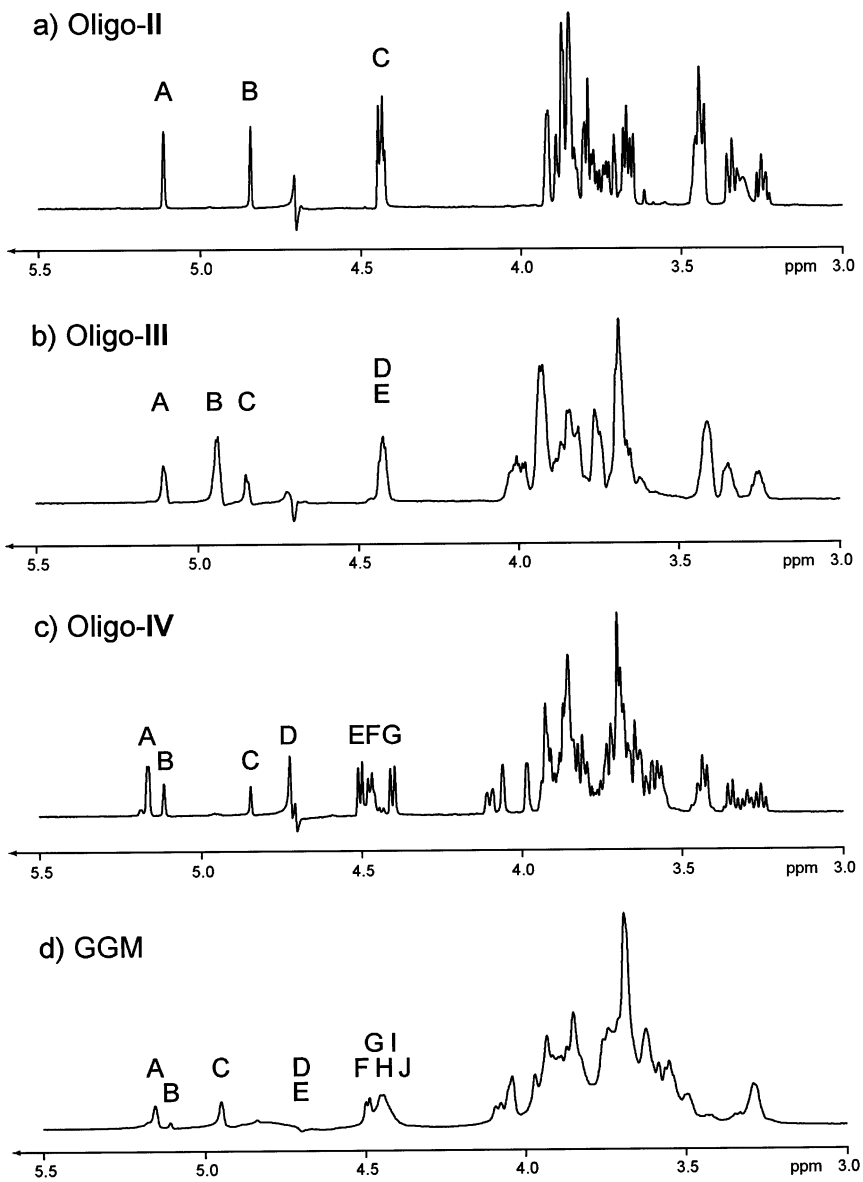

Fig. 2. 1D ^{1}H NMR spectra of (a) oligosaccharide **II**; (b) oligosaccharide **III**; (c) oligosaccharide **IV**; (d) GGM.

mined on the basis of NOESY and HMBC (Table 4).

Digestion of GGM by endo-*1,4-β-mannanase and purification of oligosaccharides **II**, **III** and **IV***.—The total degradation of GGM by *A. niger endo*-1,4-β-mannanase yielded three major peaks following gel-permeation chromatography (Fig. 4(A)). Following re-chromatography of the three major peaks, examination by HPTLC showed each to contain a single component oligosaccharide (**II**, **III**, **IV**). TLC of a total mannanase digest of GGM confirmed the presence of the same three oligosaccharides (**II**, **III**, **IV**) in addition to two minor oligosaccharides (**I**, **V**) and some trace amounts of at least two other oligosaccharides (Fig. 5, lane M) which have been eliminated during the gel-permeation chromatography steps. HPAEC-PAD confirmed this pattern (Fig. 4(B)) and established that oligosaccharides **II**, **III** and **IV** accounted for 80% of the GGM. However, HPAEC did not separate the minor oligosaccharide **V** from oligosaccharide **IV**, two compounds that were clearly separated by TLC chromatography.

*Molecular weight determination of oligosaccharides **II**, **III** and **IV***.—After positive electrospray ionisation, the underivatised oligosaccharide **IV** showed a protonated molecular ion ($[M+H]^{+}$) at m/z 991.4 and a

sodiated adduct ion ($[M+Na]^+$) at m/z 1013.4. Under the same conditions oligosaccharide **III** showed a $[M+H]^+$ ion at m/z 505.2, an adduct ion $[M+Na]^+$ at m/z 527.1 and an ion at m/z 1031.3 assigned to the structure $[2M+Na]^+$. Oligosaccharide **II** showed the complete series of adduct ions $[M+Na]^+$, $[2\,M+Na]^+$, $[3\,M+Na]^+$, $[4\,M+$

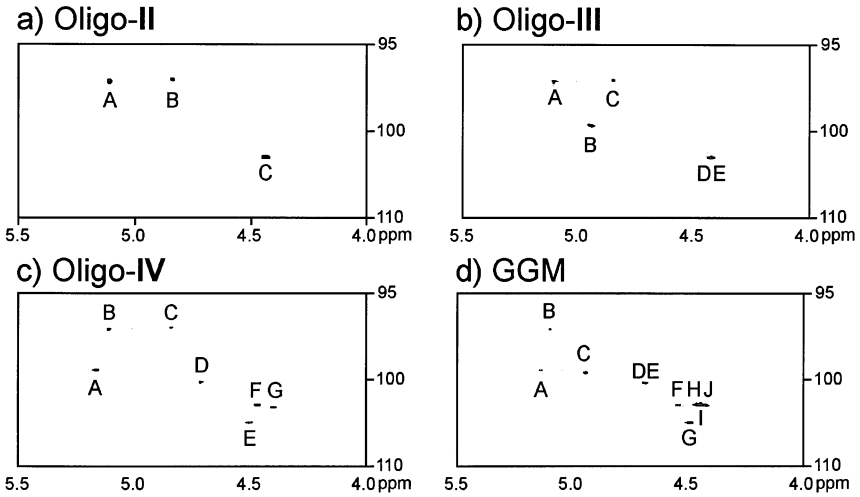

Fig. 3. Anomeric region of the HSQC of (a) oligosaccharide **II**. (b) oligosaccharide **III**. (c) oligosaccharide **IV**. (d) GGM.

Table 4
HMBC and NOESY information [a] available for the determination of interresidue correlations in GGM polysaccharide

HMBC(ω_1)	HMBC(ω_2)	NOESY(ω_1)	NOESY(ω_2)	Linkages
A(H-1)	**D**(C-6)	**A**(H-1)	**D**(H-5)	**A**-β(1→6)-**D**
A(C-1)	**D**(H-6b)	**A**(H-1)	**D**(H-6b)	α-D-Gal*p*-(1→6)-β-D-Man*p*
B(H-1)	**G**(C-4)			**B**-β(1→4)-**G**
				β-D-Man*p*-(1→4)-β-D-Glc*p*
C(H-1)	**E**(C-6)	**C**(H-1)	**E**(H-4)	
C(C-1)	**E**(H-6a)	**C**(H-1)	**E**(H-6a)	**C**-β(1→6)-**E**
C(C-1)	**E**(H-6b)	**C**(H-1)	**E**(H-6b)	α-D-Gal*p*-(1→6)-β-D-Man*p*
D(H-1)	**H**(C-4)			**D**-β(1→4)**H**
				β-D-Man*p*-(1→4)-β-D-Glc*p*
E(H-1)	**J**(C-4)	**E**(H-1)	**J**(H-3)	**E**-β(1→4)-**J**
E(C-1)	**J**(H-4)			β-D-Man*p*-(1→4)-β-D-Glc*p*
F(H-1)	**A**(C-4)			**F**-α(1→2)-**A**
				β-D-Gal*p*-(1→2)-α-D-Gal*p*
F(H-1)	**D**(C-4)	**F**(H-1)	**D**(H-3)	**F**-β(1→4)-**D**
F(C-1)	**D**(H-4)	**F**(H-1)	**D**(H-4)	β-D-Glc*p*-(1→4)-β-Man*p*
G(H-1)	**E**(C-4)	**G**(H-1)	**E**(H-3)	**G**-β(1→4)-**E**
G(C-1)	**E**(H-4)	**G**(H-1)	**E**(H-4)	β-D-Glc*p*-(1→4)-β-Man*p*
H(H-1)	**E**(C-4)	**H**(H-1)	**E**(H-3)	**H**-β(1→4)-**E**
		H(H-1)	**E**(H-4)	β-D-Glc*p*-(1→4)-β-D-Man*p*
I(H-1)	**B**(C-4)			**I**-β(1→4)-**B**
I(C-1)	**B**(H-4)			β-D-Glc*p*-(1→4)-β-D-Man*p*
J(H-1)	**B**(C-4)			**J**-β(1→4)-**B**
				β-D-Glc*p*-(1→4)-β-D-Man*p*

[a] ω_1 refers to the first (indirect) frequency dimension, while ω_2 refers to the second (direct) frequency dimension.

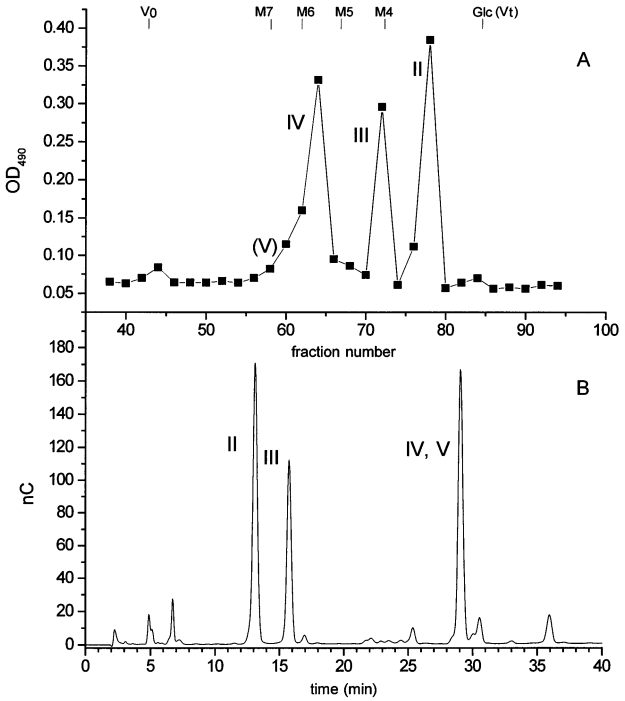

Fig. 4. Gel-permeation chromatography and anion-exchange chromatography profiles of oligosaccharides generated from *endo*-1,4-β-mannanase treatment of GGM. (A) Gel-permeation chromatography on Toyopearl HWS40. The column was calibrated with glucose and malto-oligosaccharides (DP 4–7). (B) HPAEC-PAD chromatography (CarboPac PA-1 column, Dionex).

$Na]^+$ and $[5\ M + Na]^+$ at m/z 364.8, 707.0, 1049.3, 1391.4 and 1733.6, respectively. The molecular weights of oligosaccharides **II**, **III** and **IV** were 342, 504, and 990 Da, respectively. The different patterns observed for each mass spectrum of these compounds can be explained by their respective concentrations. The more concentrated the sample, the more adduct ions were produced.

*Linkage analysis of oligosaccharides **II**, **III** and **IV**.*—Oligosaccharide **II**: Linkage analysis (Table 2) showed the presence of terminal Glc*p* and 4-Man*p* in the molar ratio of 1:1 the expected ratio for a disaccharide. The 4-mannosyl residue was the reducing end-unit. This was shown by the 1,2,3,5,6-penta-*O*-methylmannitol derivative obtained with its characteristic fragment ions at m/z 133, 157 and 205. Oligosaccharide **III**: The presence of approximately equimolar proportions of terminal Gal*p*, terminal Glc*p* and 4,6-Man*p* indicated a trisaccharide. The mannosyl residue was the reducing end-unit but was also substituted at O-6 as shown by the presence of 1,2,3,5-penta-*O*-methylmannitol with characteristic fragment ions at m/z 117, 133 and 233. Oligosaccharide **IV**: The glycosyl-linkage components were terminal Gal*p*, 2-Gal*p*, terminal Glc*p*, 4-Glc*p*, 4-Man*p*, and 4,6-Man*p* in the molar ratio of 1.3:1.3:1.2:1.2:1.0:1.1, indicating a hexasaccharide. The 4-Man*p* was at the reducing end for the reasons already stated for oligosaccharide **II**.

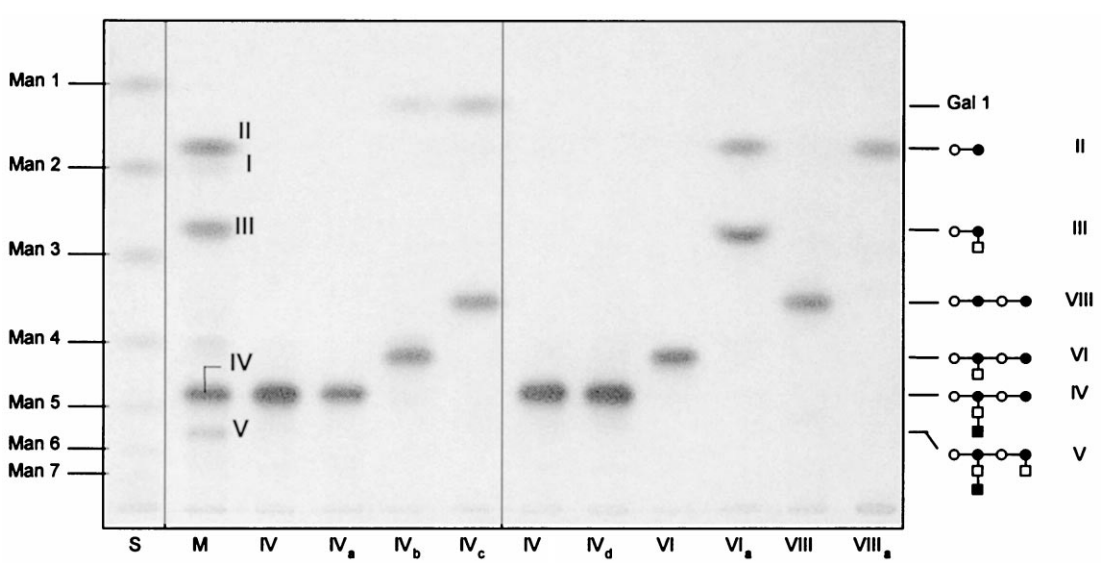

Fig. 5. Thin-layer chromatography of the enzymatic digests of GGM and oligosaccharide **IV**. Key for lanes: (S) (1→4)-β-D-mannosaccharides. (M) *endo*-1,4-β-mannanase digest of GGM. (IV) purified oligosaccharide **IV**. (IV_a) oligosaccharide **IV** + α-D-galactosidase. (IV_b) oligosaccharide **IV** + β-D-galactosidase. (IV_c) oligosaccharide **IV** + α- and β-D-galactosidases. (IV_d) oligosaccharide **IV** + *endo*-1,4-β-mannanase. (VI) purified oligosaccharide **VI**. (VI_a) oligosaccharide **VI** + *endo*-1,4-β-mannanase. (VIII) purified oligosaccharide **VIII**. ($VIII_a$) oligosaccharide **VIII** + *endo*-1,4-β-mannanase.

Table 5
^{1}H and ^{13}C NMR chemical shifts for the oligosaccharides **II**, **III** and **IV**[a,b]

Oligosaccharide		Monosaccharide residue	δ H-1 δ C-1	δ H-2 δ C-2	δ H-3 δ C-3	δ H-4 δ C-4	δ H-5 δ C-5	δ H-6a δ C-6	δ H-6b
II	**A**	→4)-α-Man^{red}	5.11 94.2	3.92 70.7	3.87 69.3	**3.80** **77.2**	3.85 71.3	3.85 60.6	3.79
	B	→4)-β-Man^{red}	4.84 94.0	3.92 71.1	3.70 72.1	**3.76** **77.2**	3.44 75.3	3.74 60.6	3.77
	C	β-D-Glc*p*-(1→	4.44 103.0	3.25 73.6	3.43 75.8	3.34 69.8	3.44 76.3	3.66 61.0	3.86
III	**A**	→4,6)-α-Man^{red}	5.11 94.2	3.92 70.5	4.03 70.0	**3.84** **77.4**	3.89 77.4	**4.00** **66.9**	**3.75**
	B	β-D-Gal*p*-(1→	4.94 99.3	3.77 68.8	3.81 69.7	3.93 71.3	3.69 71.4	n.d. [c] n.d. [c]	n.d. [c]
	C	→4,6)-β-Man^{red}	4.85 94.1	3.93 71.0	3.72 72.1	**3.77** **77.0**	3.46 76.4	3.99 66.9	3.77
	D	β-D-Glc*p*-(1→	4.42 103.0	3.30 72.3	3.62 77.1	3.26 73.6	3.76 77.1	3.80 61.4	3.95
	E	β-D-Glc*p*-(1→	4.43 103.0	3.26 73.6	3.42 75.9	3.35 69.8	3.42 76.4	3.86 61.0	3.67
IV	**A**	→2)-α-D-Gal*p*-(1→	5.17 98.9	**3.87** **78.1**	4.10 68.7	3.98 69.5	3.94 71.3	3.77 61.4	3.70
	B	→4)-α-Man^{red}	5.12 94.2	3.92 70.7	3.88 69.4	**3.80** **77.3**	3.60 71.4	3.85 60.5	3.65
	C	→4)-β-Man^{red}	4.85 103.2	3.93 74.0	3.70 75.3	**3.72** **79.7**	3.46 75.8	3.91 61.2	3.76
	D	→4,6)-β-D-Man*p*-(1→	4.73 100.3	4.06 70.4	3.86 71.5	**3.65** **77.8**	3.98 69.7	3.92 67.2	3.84
	E	β-D-Gal*p*-(1→	4.51 105.0	3.56 71.4	3.60 73.1	3.86 69.0	3.48 76.4	3.71 61.6	3.69
	F	→4)-β-D-Glc*p*-(1→	4.48 102.9	3.30 73.4	3.62 75.4	**3.68** **79.1**	3.72 71.8	3.85 60.7	3.79
	G	β-D-Glc*p*-(1→	4.41 103.2	3.25 73.6	3.43 75.8	3.34 69.9	3.45 76.4	3.86 61.0	3.67

[a] Values were determined in D_2O at 25 °C and are given in ppm relative to external [^{13}C-1]-D-glucose ($\delta_{H\text{-}1(\alpha)}$ 5.15 and $\delta_{C\text{-}1(\alpha)}$ 92.90).

[b] Chemical shifts highlighted in bold typeface indicate positions at which a glycosidic link is identified based on differences to the corresponding reference chemical shifts. [33–35]

[c] n.d. stands for 'not determined'.

*NMR spectroscopy of oligosaccharides **II**, **III** and **IV**.*—The 1D ^{1}H NMR spectra of the three oligosaccharides are shown in Fig. 2(a–c) and the assignments are given in Table 5. Oligosaccharide **II** contains three anomeric proton resonances (H-1) with relative integrals of 0.6:0.4:1 indicating a disaccharide whose reducing end has a duplicated set of resonances as a result of mutarotation. The 1D ^{1}H NMR spectrum of oligosaccharide **III** shows four H-1 resonances with integrals 0.6:1:0.4:1, consistent with a trisaccharide. The oligosaccharide **IV** spectrum has seven H-1 resonances with integrals 1:0.6:0.4:1:1:1:1 indicating an hexasaccharide. The monosaccharide units were designated **A** to **C** for oligosaccharide **II**, **A** to **D** for oligosaccharide **III** and **A** to **G** for oligosaccharide **IV,** following decreasing anomeric proton chemical shifts.

The HSQC spectra (Fig. 3(a–c)) confirmed the number of expected monosaccharide units for all three oligosaccharide samples exhibiting three anomeric resonances for the disaccharide **II** (Fig. 3(a)), five anomeric resonances for the trisaccharide **III** (Fig. 3(b)) and seven anomeric resonances for the hexasaccharide **IV** (Fig. 3(c)). In addition to the purity of the samples, the HSQC data also illustrates the

carbon shifts of the anomeric positions, an essential part of the chemical shifts' assignment process.

The anomeric ^{1}H chemical shifts and the one-bond proton-carbon scalar couplings extracted from the ω_2-undecoupled two-dimensional HMBC spectra can be used to determine the absolute anomeric (α or β) configuration of the monosaccharide units. For oligosaccharide **II**, unit **A** ($\delta_{\mathbf{A}(\text{H-1})}$ 5.11 ppm and $^1J_{\text{CH}}$ 170 Hz) is α-Hex*p* while units **B** ($\delta_{\mathbf{B}(\text{H-1})}$ 4.84 ppm and $^1J_{\text{CH}}$ 159 Hz) and **C** ($\delta_{\mathbf{C}(\text{H-1})}$ 4.44 ppm and $^1J_{\text{CH}}$ 161 Hz) are β-Hex*p*. For oligosaccharide **III**, unit **A** ($\delta_{\mathbf{A}(\text{H-1})}$ 5.11 ppm and $^1J_{\text{CH}}$ 171 Hz) is α-Hex*p* while units **B** ($\delta_{\mathbf{B}(\text{H-1})}$ 4.94 ppm and $^1J_{\text{CH}}$ 169 Hz), **C** ($\delta_{\mathbf{C}(\text{H-1})}$ 4.85 ppm and $^1J_{\text{CH}}$ 159 Hz), **D** ($\delta_{\mathbf{D}(\text{H-1})}$ 4.43 ppm and $^1J_{\text{CH}}$ 162 Hz) and **E** ($\delta_{\mathbf{E}(\text{H-1})}$ 4.42 ppm and $^1J_{\text{CH}}$ 162 Hz) are β-Hex*p*. For oligosaccharide **IV**, units **A** ($\delta_{\mathbf{A}(\text{H-1})}$ 5.17 ppm and $^1J_{\text{CH}}$ 174 Hz) and **B** ($\delta_{\mathbf{B}(\text{H}-1)}$ 5.12 ppm and $^1J_{\text{CH}}$ 170 Hz) are α-Hex*p* while units **C** ($\delta_{\mathbf{C}(\text{H-1})}$ 4.85 ppm and $^1J_{\text{CH}}$ 161 Hz), **D** ($\delta_{\mathbf{D}(\text{H-1})}$ 4.73 ppm and $^1J_{\text{CH}}$ 161 Hz), **E** ($\delta_{\mathbf{E}(\text{H-1})}$ 4.51 ppm and $^1J_{\text{CH}}$ 162 Hz), **F** ($\delta_{\mathbf{F}(\text{H-1})}$ 4.48 ppm and $^1J_{\text{CH}}$ 163 Hz) and **G** ($\delta_{\mathbf{G}(\text{H-1})}$ 4.41 ppm and $^1J_{\text{CH}}$ 162 Hz) are β-Hex*p*.

Table 6
HMBC information [a] available for the determination of inter-residue correlations in the oligosaccharides **II**, **III** and **IV**

Oligo-saccharide	ω_1	ω_2	Linkages
II	**A**(H-4)	**C**(C-1)	**C**-α(1→4)-**A**
	A(C-4)	**C**(H-1)	β-D-Glc*p*-(1→4)-α-Man^{red}
	B(H-4)	**C**(C-1)	**C**-β(1→4)-**B**
	B(C-4)	**C**(H-1)	β-D-Glc*p*-(1→4)-β-Man^{red}
III	**A**(H-6a)	**B**(C-1)	
	A(H-6b)	**B**(C-1)	**B**-α(1→6)-**A**
	A(C-6)	**B**(H-1)	β-D-Gal*p*-(1→6)-α-Man^{red}
	C(H-6a)	**B**(C-1)	
	C(H-6b)	**B**(C-1)	**B**-β(1→6)-**C**
	C(C-6)	**B**(H-1)	β-D-Gal*p*-(1→6)-β-Man^{red}
	D(H-1)	**A**(C-4)	**D**-α(1→4)-**A**
	D(C-1)	**A**(H-4)	β-D-Glc*p*-(1→4)-α-Man^{red}
	D(H-1)	**C**(C-4)	**D**-β(1→4)-C
	D(C-1)	**C**(H-4)	β-D-Glc*p*-(1→4)-β-Man^{red}
	E(H-1)	**A**(C-4)	**E**-α(1→4)-**A**
	E(C-1)	**A**(H-4)	β-D-Glc*p*-(1→4)-α-Man^{red}
	E(H-1)	**C**(C-4)	**E**-β(1→4)-**C**
	E(C-1)	**C**(H-4)	β-D-Glc*p*-(1→4)-β-Man^{red}
IV	**A**(H-1)	**D**(C-6)	
	A(C-1)	**D**(H-6a)	**A**-β(1→6)-**D**
	A(C-1)	**D**(H-6b)	α-D-Gal*p*-(1→6)-β-D-Man*p*
	D(H-1)	**F**(C-4)	**D**-β(1→4)-**F**
	D(C-1)	**F**(H-4)	β-D-Man*p*-(1→4)-β-D-Glc*p*
	E(H-1)	**A**(C-2)	**E**-α(1→2)-**A**
	E(C-1)	**A**(H-2)	β-D-Gal*p*-(1→2)-α-D-Gal*p*
	F(H-1)	**B**(C-4)	**F**-α(1→4)-**B**
	F(C-1)	**B**(H-4)	β-D-Glc*p*-(1→4)-α-Man^{red}
	F(H-1)	**C**(C-4)	**F**-β(1→4)-**C**
	F(C-1)	**C**(H-4)	β-D-Glc*p*-(1→4)-β-Man^{red}
	G(H-1)	**D**(C-4)	**G**-β(1→4)-**D**
	G(C-1)	**D**(H-4)	β-D-Glc*p*-(1→4)-β-D-Man*p*

[a] ω_1 refers to the first (indirect) frequency dimension, while ω_2 refers to the second (direct) frequency dimension.

The glycosidic linkages between monosaccharide units were determined for all three oligosaccharide samples on the basis of NOESY and HMBC (Table 6).

Enzymatic analyses of GGM oligosaccharides.—After complete enzymatic digestion of GGM with *endo*-1,4-β-D-mannanase, at least 80% of the GGM derived products were found in oligosaccharides **II**, **III** and **IV**, in the molar ratio of 2:1:1 respectively. The reported data have provided conclusive evidence for the structural assignments outlined in Table 7. Each oligosaccharide contained an even number of backbone glycosyl residues with alternating Glc-Man residues with the mannosyl residue always located at the reducing end. Only traces of mannobiose (**I**) were detected (Fig. 5, lane M; identified by its R_f value) indicating that the GGM backbone is predominantly composed of alternating sequences of Glc-Man residues.

The anomeric configurations of the Gal*p* residues present in oligosaccharide **IV** were confirmed by digestion with α- and β-D-galactosidases (Fig. 5). The purified oligosaccharide was insensitive to the action of α-D-galactosidase from green coffee bean but was hydrolysed by β-D-galactosidase from *A. niger*, indicating that the terminal Gal*p* was in the β configuration. Reaction products were galactose and an oligosaccharide presumed to be β-D-Glc*p*-(1→4)-[α-D-Gal*p*-(1→6)]-β-D-Man*p*-(1→4)-β-D-Glc*p*-(1→4)-β-D-Man*p*-(1→ (structure **VI**). Enzymatic hydrolysis of compound **IV** using both β- and α-D-galactosidase yielded galactose and the linear oligosaccharide β-D-Glc*p*-(1→4)-β-D-Man*p*-

Table 7
Structure of oligosaccharides generated by enzymatic digestion of: (a) GGM (oligosaccharides **I–V**). (b) Oligosaccharides **IV**, **V** and **VI** (oligosaccharides **VI–VIII**)

Structure No	*Relative amount %	Compound	Substrate	Enzyme
I		β-D-Man*p*-(1→4)-β-D-Man*p*-(1→	GGM	β--mannanase
II	31.3	β-D-Glc*p*-(1→4)-β-D-Man*p*-(1→	GGM	β--mannanase
III	20.1	β-D-Glc*p*-(1→4)-[α-D-Gal*p*-(1→6)]-β-D-Man*p*-(1→	GGM	β-mannanase
IV	29.2	β-D-Glc*p*-(1→4)-[β-D-Gal*p*-(1→2)-α-D-Gal*p*-(1→6)]-β-D-Man*p*-(1→4)-β-D-Glc*p*-(1→4)-β-D-Man*p*-(1→	GGM	β-mannanase
V		β-D-Glc*p*-(1→4)-[β-D-Gal*p*-(1→2)-α-D-Gal*p*-(1→6)]-β-D-Man*p*-(1→4)-β-D-Glc*p*-(1→4)-[α-D-Gal*p*-(1→6)]-β-D-Man*p*-(1→	GGM	β-mannanase
VI		β-D-Glc*p*-(1→ 4)-[α-D-Gal*p*-(1→ 6)]-β-D-Man*p*-(1→4)-β-D-Glc*p*-(1→4)-β-D-Man*p*-(1→	IV	β-galactosidase
VII		β-D-Glc*p*-(1→ 4)-[α-D-Gal*p*-(1→ 6)]-β-D-Man*p*-(1→4)-β-D-Glc*p*-(1→4)-[α-D-Gal*p*-(1→6)]-β-D-Man*p*-(1→	V	β-galactosidase
VIII		β-D-Glc*p*-(1→4)-β-D-Man*p*-(1→4)-β-D-Glc*p*-(1→4)-β-D-Man*p*-(1→	VI	α-galactosidase

* Calculated from peak areas of individual components from anion-exchange HPLC

(1→4)-β-D-Glc*p*-(1→4)-β-D-Man*p*-(1→ (structure **VIII**) indicating that the Gal*p* residue attached to the backbone was in α configuration. It should be mentioned that only α-D-galactosidase from coffee bean was able to remove the terminal α-Gal*p* from structure **VI** in contrast to α-D-galactosidase from *A. niger* which was totally ineffective, probably because the binding requirements of these enzymes differ according to the residues linked to the terminal α-D-Gal*p*.

The reaction products obtained from *A. niger endo*-1,4-β-D-mannanase action on these two oligosaccharides were consistent with their presumed structures (Fig. 5): β-D-Glc*p*-(1→4)-[α-D-Gal*p*-(1→6)]-β-D-Man*p*-(1→ (structure **III**) and β-D-Glc*p*-(1→4)-β-D-Man*p*-(1→ (structure **II**) were produced from oligosaccharide **VI** whereas only β-D-Glc*p*-(1→4)-D-β-Man*p*-(1→ was formed by *endo*-1,4-β-D-mannanase action on oligosaccharide **VIII**. *Endo*-1,4-β-D-mannanase was unable to cleave oligosaccharide **IV** indicating that the terminal β-Gal*p* prevents the enzyme from binding to the backbone glycosyl residues of the oligosaccharide.

The structure of the minor oligosaccharide **V** was deduced from the products obtained by enzymatic digestion (Fig. 6). β-D-Galactosidase yielded galactose and an oligosaccharide presumed to be β-D-Glc*p*-(1→4)-[α-D-Gal*p*-(1→6)]-β-D-Man*p*-(1→4)-β-D-Glc*p*-(1→4)-[α-D-Gal*p*-(1→6)]-β-D-Man*p*-(1→ (structure

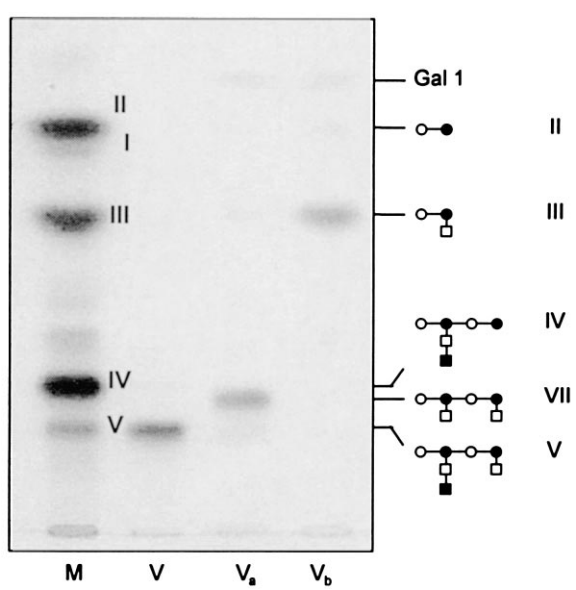

Fig. 6. Thin-layer chromatography of the enzyme digests of GGM and oligosaccharide **V**. Key for lanes: (M) *endo*-1,4-β-mannanase digest of GGM. (V) purified oligosaccharide **V**. (V_a) oligosaccharide **V** + β-D-galactosidase. (V_b) oligosaccharide **V** + β-D-galactosidase and *endo*-1,4-β-mannanase.

VII) since only the oligosaccharide β-D-Glc*p*-(1→4)-[α-D-Gal*p*-(1→6)]-β-D-Man*p*-(1→ (structure **III**) was produced upon further hydrolysis with *endo*-1,4-β-D-mannanase.

4. Conclusions

The major structural features of a GGM have been characterised following isolation and purification of the polysaccharide from the outer pericarp of ripe kiwifruit. Ripe fruit were used as the source of GGM for two reasons. Starch, which in unripe kiwifruit is present at four times the level of the cell wall material, almost disappears during ripening allowing a more straightforward extraction protocol to be used for the isolation of cell wall material. Secondly, the pectic polysaccharides were in an advanced state of degradation, which meant that the compact integrated structure of the primary cell wall found in unripe fruit became much more open and swollen, making non-cellulosic polysaccharides more amenable to chemical extraction. The structure of GGM appears to remain unchanged during kiwifruit ripening with regard to both its primary sequence and molecular weight.[36] Nevertheless, it could be argued that some inadvertent degradation of the GGM occurred during the initial extraction step in cold water. However, two things suggest this did not occur. The final Gal–Glc–Man ratio was identical to that reported for GGM isolated from unripe kiwifruit by a protocol which inhibited all endogenous enzyme activity. Moreover, during the initial extraction step, the pH of the homogenate was 3.5, well below the pH optimum for kiwifruit β-galactosidase action on cell wall substrates.[37]

Kiwifruit GGM contained Gal–Glc–Man in the ratio of 1:2:2 which was characteristic for GGM previously reported for kiwifruit.[13] The backbone was predominantly alternating →4)-β-D-Man*p*-(1→ and →4)-β-D-Glc*p*-(1→ residues. Approximately 35% of the mannose residues carried substituents which were either single α-D-Gal*p*-(1→ residues (50% of branches) or the disaccharide β-D-Gal*p*-(1→2)-α-D-Gal*p*-(1→ (50% of branches). Most of the GGM (80%) consisted of oligosaccharides **II**, **III** and **IV** in addition to smaller amounts of **I** and **V**.

While kiwifruit GGM had several features in common with the GGM characterised by Sims et al.[18] from the extracellular medium of suspension cultures of *N. plumbaginifolia*, there were several important differences. Sims and co-workers confirmed the presence of arabinose and xylose, both as components of the GGM polysaccharide and of specific oligosaccharides derived from it. In kiwifruit GGM, although trace amounts of xylose, arabinose and fucose were present, and terminal xylose was detected in the linkage analysis, none of these sugars were detected as components of any oligosaccharide derived from GGM following enzymatic hydrolysis. Therefore, the trace of terminal xylose is likely to be derived from a trace contaminant of xyloglucan. Nevertheless, it should be pointed out that we have previously shown that a partially purified GGM from suspension cultured kiwifruit cells contained 3.3 and 1.5 mol.% terminal arabinosyl and xylosyl residues respectively.[13] This level of arabinose in particular, is too high to be derived from contaminating xyloglucan and suggests that it is a valid component of the GGM isolated from suspension cultured cells.

The backbone of kiwifruit GGM was less highly branched than that of GGM from *N. plumbaginifolia*.[18] This was confirmed by the different ratios of oligosaccharides formed following *endo*-1,4-β-mannanase treatment of the respective GGMs. GGM from *N. plumbaginifolia* contained only 10% of its structure as the disaccharide β-D-Glc*p*-(1→4)-β-D-Man*p*-(1→ whereas in kiwifuit it accounted for nearly 30% of the GGM structure. The major oligosaccharide in GGM from *N. plumbaginifolia* (27%) was a heptasaccharide identical to oligosaccharide **V,** a minor constituent of kiwifruit GGM.

The action of *A. niger endo*-1,4-β-mannanase on kiwifruit GGM is consistent with the mechanisms deduced from the enzymatic breakdown of glucomannans and galactomannans. Extensive studies[38] have shown that *endo*-1,4-β-mannanases have five binding-subsites labelled from −3 to +2 with cleavage

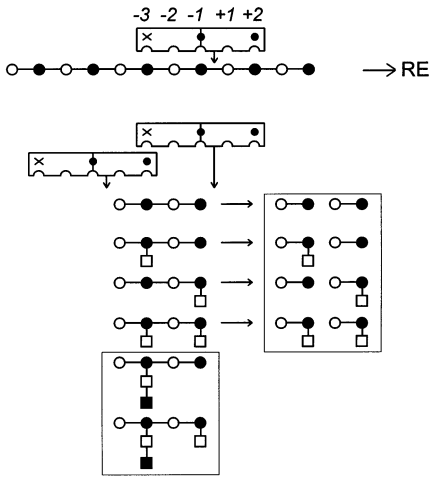

Fig. 7. Proposed binding mechanism based on the main oligosaccharides released on reaction of *A. niger endo*-1,4-β-mannanase and GGM from kiwifruit. (a) Schematic representation of subsite binding. (b) All possible oligosaccharides containing 4 or 2 backbone residues. End products are outlined. Symbolic notations for the enzyme: ● must be mannose; | must be unsubstituted or substituted with only the monogalactosyl (α-Gal*p*) residue; × binding not essential.

taking place between −1 and +1 subsites.[39] In the case of *A. niger endo*-1,4-β-mannanase, the requirement for binding at the −3 subsite is not essential. Hydrolysis of deacetylated salep glucomannan has shown that the enzyme requires mannosyl residues in subsites −1 and +2. In contrast, the pyranose rings in subsites −2 and +1 can be glucosyl or mannosyl residues but galactosyl substitution at these residues blocks the hydrolysis.

The binding mechanism of *A. niger endo*-1,4-β-mannanase to GGM is proposed in Fig. 7. If we assume that the backbone is composed of alternating Glc-Man residues in which only mannose is substituted with mono- or digalactosyl residues, then subsites −1 and +2 bind to evenly spaced mannosyl residues. There is no hindrance at the binding sites −2 and +1 since the corresponding glucosyl residues are never substituted. As hydrolysis cannot occur if the mannosyl residue at subsite −1 is substituted with β-D-Gal*p*-(1→2)-α-D-Gal*p*-(1→ residues, an additional requirement is that this mannosyl residue must be either unsubstituted or substituted with only one galactosyl residue (α-D-Gal*p*).

All possible oligosaccharides containing four or two backbone residues that could be produced according to this scheme are shown in Fig. 7. The four possible end products (structures **II**, **III**, **IV**, **V**) have been found as components in the *endo*-1,4-β-mannanase digests of GGM. In contrast, oligosaccharides with digalactosyl substitution on the reducing mannosyl residue cannot be produced and have not been detected.

It is not possible from this study to define the complete primary sequence of kiwifruit GGM. A structure based solely on oligosaccharides **II**, **III** and **IV** would be invalid, because it ignores the fact that the three oligosaccharides do not account for 100% of the GGM, and does not take into account the additional presence of mannobiose (**I**) and oligosaccharide **V**. Nevertheless, the restricted number of peaks present in the NMR polysaccharide spectra, and the fact that a vast majority of the glycosidic linkages identified can be adequately described by a regular structure, suggests that for the most part, kiwifruit GGM consists of sequences composed of the three oligosaccharides **II**, **III** and **IV**. It is concluded that kiwifruit GGM consists, for the most part, of an alternating glucose-mannose backbone with 35% of the mannose residues substituted alternately with one or two galactose residues, the substituted residues being separated by either three or five unsubstituted monosaccharide units.

Acknowledgements

We wish to thank Laurent Fay (Nestlé) for the molecular weight determination of the oligosaccharides, Eric Koh (HortResearch) for the molecular weight measurements of the GGM, and Heather Baker (School of Biological Sciences, Auckland, NZ) for the use of the dynamic laser-light scattering spectrometer.

References

[1] Bacic, A.; Harris, P. J.; Stone, B. A. In *The Biochemistry of Plants*; Priess, J., Ed.; Academic: New York, 1988; Vol. 14, pp. 297–371.
[2] Hayashi, T. *Ann. Rev. Plant Phys. Plant Mol. Biol.* **1989**, *40*, 139–168.
[3] Fry, S. C.; Smith, R. C.; Renwick, K. F.; Martin, D. J.; Hodge, S. K.; Matthews, K. J. *Biochem. J.* **1992**, *282*, 821–828.
[4] Thompson, J. E.; Smith, R. C.; Fry, S. C. *Biochem. J.* **1997**, *327*, 699–708.

[5] Geddes, D. S.; Wilkie, K. C. B. *Carbohydr. Res.* **1972**, *23*, 349–357.
[6] Bremner, I.; Wilkie, K. C. B. *Carbohydr. Res.* **1971**, *20*, 193–203.
[7] Wenda, L.; Peiqing, W.; Pinyu, L.; Wood, J. *Chem. Tech.* **1990**, *10*, 123–132.
[8] Tenkanen, M.; Makkonen, M.; Perttula, M.; Viikari, L.; Teleman, A. *J. Biotechnol.* **1997**, *57*, 191–204.
[9] Kubacková, M.; Karácsonyi, Š.; Bilisics, L. *Carbohydr. Polym.* **1992**, *19*, 125–129.
[10] Jakimow-Barras, N. *Phytochemistry* **1973**, *12*, 1331–1339.
[11] Eda, S.; Akiyama, Y.; Kato, K.; Takahashi, R.; Kusakabe, I.; Ishizu, A.; Nakano, J. *Carbohydr. Res.* **1984**, *131*, 105–118.
[12] Alam, M.; Richards, G. N. *Aust. J. Chem.* **1971**, *24*, 2411–2416.
[13] Fischer, M.; Wegzryn, T. F.; Hallett, I. C.; Redgwell, R. J. *Carbohydr. Res.* **1996**, *295*, 195–208.
[14] Eda, S.; Akayama, Y.; Kato, K. *Carbohydr. Res.* **1985**, *137*, 173–182.
[15] Cartier, N.; Chambat, G.; Joseleau, J-P. *Phytochemistry* **1988**, *27*, 1361–1364.
[16] Akiyama, Y.; Eda, S.; Mori, M.; Kato, K. *Phytochemistry* **1983**, *22*, 1177–1180.
[17] Akiyama, Y.; Kato, K. *Phytochemistry* **1982**, *21*, 1325–1329.
[18] Sims, I. M.; Craik, D. J.; Bacic, A. *Carbohydr. Res.* **1997**, *303*, 79–92.
[19] Ciucanu, I.; Kerek, F. *Carbohydr. Res.* **1984**, *131*, 209–217.
[20] Dubois, M.; Gilles, K. A.; Hamilton, J. K.; Rebers, P. A.; Smith, F. *Anal. Chem.* **1956**, *28*, 350–356.
[21] Hansen, S. A. *J. Chromatogr.* **1975**, *105*, 388–390.
[22] Marion, D.; Wüthrich, K. *Biochem. Biophys. Res. Commun.* **1983**, *113*, 967–974.
[23] Piantini, U.; Sørensen, O. W.; Ernst, R. R. *J. Am. Chem. Soc.* **1982**, *104*, 6800–6801.
[24] Rance, M.; Sørensen, O. W.; Bodenhausen, G.; Wagner, G.; Ernst, R. R.; Wüthrich, K. *Biochem. Biophys. Res. Commun.* **1983**, *117*, 479–485.
[25] Braunschweiler, L.; Ernst, R. R. *J. Magn. Reson.* **1983**, *53*, 521–528.
[26] Jeener, J.; Meier, B. H.; Bachmann, P.; Ernst, R. R. *J. Chem. Phys.* **1979**, *11*, 4546–4553.
[27] Kumar, A.; Ernst, R. R.; Wüthrich, K. *Biochem. Biophys. Res. Commun.* **1980**, *95*, 1–6.
[28] Kay, L. E.; Keifer, P.; Saarinen, T. *J. Am. Chem. Soc.* **1992**, *114*, 10663–10665.
[29] Bax, A.; Summers, M. F. *J. Am. Chem. Soc.* **1986**, *108*, 2093–2094.
[30] Meier, H. *Acta Chem. Scand.* **1960**, *14*, 749–756.
[31] Ruperez, P.; Selvendran, R. R.; Stevens, B. J. H. *Carbohydr. Res.* **1985**, *142*, 107–113.
[32] Redgwell, R. J.; Melton, L. D.; Brasch, D. J. *Plant Phys.* **1992**, *98*, 71–81.
[33] Bock, K.; Thøgersen, H. *Annu. Rep. NMR Spectrosc.* **1982**, *13*, 1–57.
[34] Bock, K.; Pedersen, C. *Adv. Carbohydr. Chem. Biochem.* **1983**, *41*, 27–66.
[35] Bock, K.; Pedersen, C.; Pedersen, H. *Adv. Carbohydr. Chem. Biochem.* **1983**, *42*, 193–225.
[36] Redgwell, R. J.; Melton, L. D.; Brasch, D. J. *Carbohydr. Res.* **1991**, *209*, 191–202.
[37] Ross, G. S.; Redgwell, R. J.; MacRae, E. A. *Planta* **1993**, *189*, 499–506.
[38] McCleary, B. V.; Matheson, N. K. *Carbohydr. Res.* **1983**, *119*, 191–219.
[39] Davies, G. J.; Wilson, K. S.; Henrissat, B. *Biochem. J.* **1997**, *321*, 557–559.